



Thermomechanical analysis of the new ferromagnetic MAX-phase compound Mn_2VSnC_2 : Insights from DFT calculations

I OUADHA¹, A AZZOUZ-RACHED¹, H RACHED^{1,2} *, A BENTOUAF^{3,4}, D RACHED¹ and S AL-QAISI⁵

¹Magnetic Materials Laboratory (LMM), Faculty of Exact Sciences, Djillali Liabès University of Sidi Bel-Abbès (UDL), Sidi Bel-Abbès, Algeria

²Department of Physics, Faculty of Exact Sciences and Informatics (FSEI), Hassiba Benbouali University of Chlef (UHBC), Chlef, Algeria

³Laboratory of Physical Chemistry of Advanced Materials (LPCMA), Djillali Liabès University of Sidi Bel-Abbès (UDL), Sidi Bel-Abbès, Algeria

⁴Faculty of Technology, Dr Moulay Tahar University of Saida, Saida, Algeria

⁵Palestinian Ministry of Education and Higher Education, Nablus, Palestine

*Corresponding author. E-mail: habib_rached@yahoo.fr

MS received 13 April 2022; revised 29 August 2022; accepted 3 November 2022

Abstract. MAX-phase compounds have recently gained increased technical interest owing to their distinctive characteristics that combine the inherent properties of metals and ceramics, making them suitable for various high-level industrial applications. Based on this vision, we report a detailed theoretical study of a new quaternary ferromagnetic MAX-phase compound Mn_2VSnC_2 . We found that Mn_2VSnC_2 is mechanically and thermodynamically stable in α -polymorph ferromagnetic ordering. The macroscopic mechanical properties showed that Mn_2VSnC_2 was ductile (i.e., tolerant to damage). The obtained high melting and Debye temperatures validated the possible application of Mn_2VSnC_2 in harsh environmental applications. The electronic structures revealed that this compound exhibited metallic behaviour. Furthermore, we analysed the effects of pressure and temperature on different properties. Finally, the findings established that the title compound has good thermomechanical efficiency.

Keywords. Quaternary MAX-phases; Mn_2VSnC_2 compound; ferromagnetic ordering; *ab-initio* calculations; thermomechanical efficiency.

PACS Nos 04.20.Hr; 80.98.Hb; 20.12.Dl

1. Introduction

MAX phases have attracted the attention of chemists, physicists and technicians because of their exceptional qualities [1]. The first study of this type of compound family was conducted on Ti_3SiC_2 powder in the 1960s [2]. Attention to the MAX phases has intensified since the mid-1990s when the intrinsic properties of the compounds were recognised [3,4]. Many new MAX-phase compounds were synthesised in bulk and thin-film forms [5]. In general, this family of compounds exhibits high hardness, electrical conductivity, melting temperature and thermal shock resistance [6,7]. These interesting features are due to the combination of metallic and covalent bonds between different atomic layers [8]. Recently, MAX-phase compounds have been employed in various

industrial applications such as high-temperature structural applications, medical devices, portable electronic devices, automobiles, aerospace, defence, sensors, electrical contacts, thermal barrier coatings and protective coatings [9].

The MAX-phase compounds crystallise in a hexagonal structure with space group $P6_3/mmc$ ($N^{\circ}194$) [9]. Their structure consists of $(n + 1)$ ceramic $M_{n+1}X_n$ layers intercalated between metallic A-group element layers of one-atom-thickness (M is an early transition-metal element, X is C and/or N element and $n = 1-3$) [10]. More recent research on these materials has focussed on the magnetic ordering of MAX-phase compounds. In addition to their desirable mechanical properties, these materials have a nanostratified structure, where M_2X layers are sandwiched between A layers, including

transcending conventional ferromagnetic, ferrimagnetic and antiferromagnetic ordering [11]. Since 2013, systematic theoretical and experimental research has led to the discovery of new magnetic MAX-phase compounds, such as the ternary compounds Mn_2SiC [11], Ta_2TlX (X: C or N) [12], M_3GaC_2 (M: Ti or Zr) [13], Cr_2AlC [14,15], Mn_2GaC [16], Mn_2AlC and Cr_2GaC [17] and quaternary $(\text{MoMn})_2\text{GaC}$ [18,19] and $(\text{VMn})_3\text{GaC}_2$ [20]. First, in this theoretical report, we used DFT calculations to study the structural properties of the quaternary MAX-phase compound Mn_2VSnC_2 in different magnetic configurations to predict the equilibrium ground-state properties. Second, we investigated the elastic, electronic and thermodynamic properties of this compound to explore its thermomechanical efficiency.

2. Computational method

All our calculations were done using the plane-wave method FP-LAPW, as implemented in the WIEN2K code [21,22], and we adopted the LSDA of Perdew and Wang [23] to determine the exchange-correlation (XC) potentials of electrons. The MT sphere radius (R_{MT}) for Mn, V, Sn and C elements are 2.14, 1.92, 2.5 and 1.49 Bohr, respectively. According to the convergence tests, the $R_{\text{MT}} \times K_{\text{max}}$ parameter was set to 8, whereas the Fourier-expanded charge density G_{max} was set to 14 for all our calculations. The self-consistent field (SCF) cycle was performed iteratively until a convergence energy of 0.00001 Ry was reached. The charge convergence was set to 0.00001 e/Bohr³. The Monkhorst–Pack method was employed with 200 special k -points on the irreducible Brillouin zone (IBZ) [24]. The separation energy was chosen as -7 Ry (Rydberg) to separate the valence and core states.

3. The crystal structure and equilibrium ground-state properties

The MAX-phase materials crystallise in the $\text{P6}_3/\text{mmc}$ space group with two different potential Wyckoff positions, called α - and β -polymorph-type structures (see table 1) [25], whose primitive cell has 12 atoms, where the internal parameters Z_{M} and Z_{C} are specific to the M and C atoms, respectively. To determine which of the two possible structures and in which magnetic configurations the studied compound is stable (see figure 1, α -polymorph (upper panel) and β -polymorph (lower panel)), we calculated the total energies as a function of the unit-cell volume of α - and β -polymorphs for the non-magnetic, FM and AFM orders, which are shown in figure 2. The calculated total energies were fitted

Table 1. The Wyckoff positions of the Mn_2VSnC_2 compound.

		Wyckoff coordinates				
		α -polymorph				
Atom	Site	x	y	z	Z_i	
$\text{M}_I(\text{V})$	$4f$	0	0	0		
$\text{M}_{II}(\text{Mn})$	$2a$	$\frac{1}{3}$	$\frac{2}{3}$	Z_{M}		0.11257875
A(Sn)	$2d$	0	0	$\frac{1}{4}$		
X(C)	$4f$	$\frac{2}{3}$	$\frac{1}{3}$	Z_{C}		0.07109359
		Wyckoff coordinates				
		β -polymorph				
Atom	Site	x	y	z	Z_i -range	
$\text{M}_I(\text{V})$	$4f$	0	0	0		
$\text{M}_{II}(\text{Mn})$	$2a$	$\frac{1}{3}$	$\frac{2}{3}$	Z_{M}		0.10385612
A(Sn)	$2d$	$\frac{1}{3}$	$\frac{2}{3}$	$\frac{1}{4}$		
X(C)	$4f$	$\frac{2}{3}$	$\frac{1}{3}$	Z_{C}		0.06701071

using Birch–Murnaghan’s equation of state (EOS) to determine the equilibrium ground-state properties, such as lattice parameters, ground-state energy of the system and bulk modulus. Figure 2 shows that the total energy of the FM α -polymorph phase is lower than that for the other phases, indicating that our compound is stabilising in the α -polymorph structure with a ferromagnetic configuration. The calculated equilibrium ground-state properties of Mn_2VSnC_2 are summarised in table 2. From these results, we observe that the structural results agree with those of the ternary V_3SnC_2 compound.

We have also calculated the formation energy, which is the best indicator that provides information about thermodynamic stability [26,27]. The calculated formation energies are also listed in table 2. The formation energy is negative, indicating that the test compound is thermodynamically stable. In addition, we have analysed the dynamic stability of our compound by calculating the phonon band structure. This calculation was performed using the CASTEP code based on the density functional perturbation theory (DFPT) [28,29]. The finite displacement method was chosen for calculating phonon frequencies [30] and we have adopted a supercell containing eight primitive cells. Figure 3 displays the obtained phonon band structures along the high symmetry directions in the first BZ. There are 12 atoms in the primitive cell, while the phonon dispersion

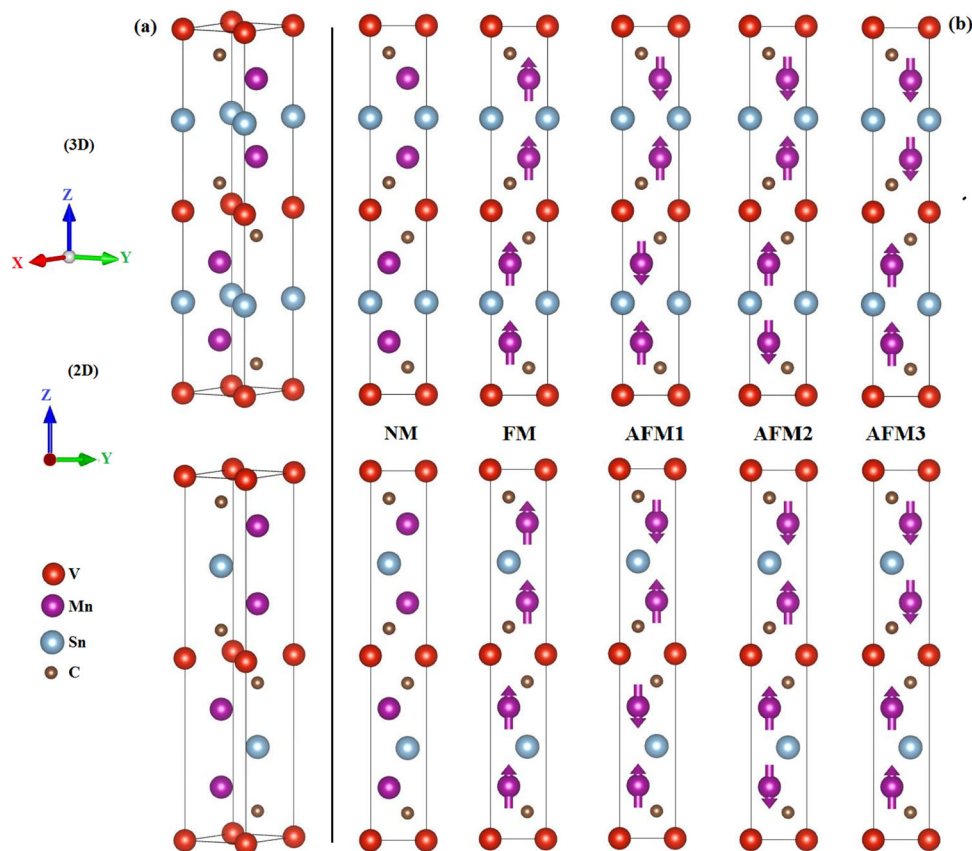


Figure 1. (a) A view of the crystal structure for α - and β -polymorphs, (b) the magnetic ordering configurations for α - and β -polymorphs, where α corresponds to the upper panel and β to the lower panel.

graph contains 36 branches consisting of 12 acoustic and 24 optic branches. The branches do not have the imaginary part, which confirms the dynamical stability of the compound.

As Mn_2VSnC_2 is ferromagnetic, we have also evaluated the total and atomic magnetic moments (M_{tot} and M_{atomic}) reported in table 3. The total magnetic moment of the compound is equal to the sum of all individual M_{atomic} of the primary cell (Mn: 4 atoms, V: 2 atoms, Sn: 2 atoms and C: 4 atoms) and those of the interstitial regions. M_{tot} of Mn_2VSnC_2 is approximately $7.4 \mu_B$ at zero pressure. We mention here that the contribution of the Mn atom is more significant in M_{tot} than the contribution of the other atoms constituting the compound.

4. Mechanical characteristics

The study of the mechanical properties of the material, which are closely related to the elastic constants, is very important to determine the prospects for its application in a particular technical field. The calculation of the elastic constants can inform us about the isotropy, anisotropy, type of bonds, stiffness, hardness, brittleness (or ductility) and the stability of the crystal structure

of the materials. We have employed the Hex-elastic-package by Jamal Morteza *et al* to calculate those elastic constants. Further details about this package are given in [31–33]. In the hexagonal system, there are five independent elastic constants, C_{11} , C_{12} , C_{13} , C_{33} and C_{44} and the sixth coefficient is computed using the equation $C_{66} = (C_{11} - C_{12})/2$. To confirm the mechanical stability of the materials, these constants must meet the condition stability criteria [34]:

$$\begin{cases} C_{11} > |C_{12}|, 2C_{13}^2 < C_{33}(C_{11} + C_{12}) \\ C_{44} > 0, C_{66} > 0 \end{cases} \quad (1)$$

Table 4 shows our results relating to the calculation of the elastic constants of our compound Mn_2VSnC_2 and another theoretical result recently obtained for the ternary V_3SnC_2 MAX-phase compound. We can observe that all the calculated elastic constants for the Mn_2VSnC_2 compound are positive and fulfil the conditions of mechanical stability. They correspond to the values calculated for their counterparts of the same V_3SnC_2 MAX-phase family, indicating that the studied material is mechanically stable against elastic deformations. Note that the value of C_{33} is less than C_{11} , indicating that the c -axis is more compressible than the other axes. We can calculate the macroscopic elastic

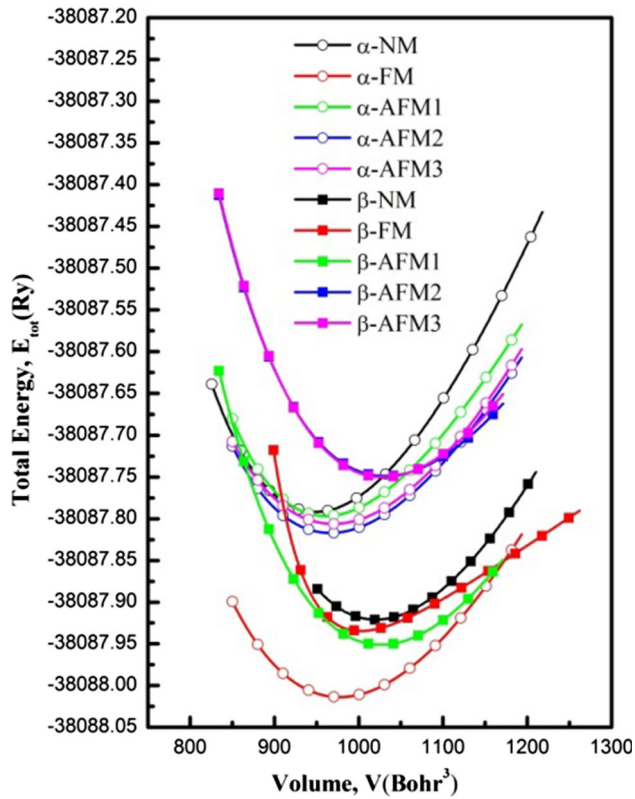


Figure 2. Total energy as a function of the unit cell volume for Mn_2VSnC_2 .

moduli, such as the bulk, shear, Young's moduli and Poisson's ratio from the elastic constants and according to the Voigt–Reuss–Hill approximations for the polycrystalline hexagonal crystal system [35–38]. The predicted values for parameters B , G , E and ν are listed in table 5. From these data, we note that all our values

agree with the compared values of the ternary compound reported in the same table. Furthermore, in mechanical engineering, hardness is one of the very important macroscopic mechanical properties of materials and it expresses the resistance of the material to corrosion, which means harder materials are more resistant to corrosion. The theoretical Vickers's hardness function is closely related to the bulk and shear moduli of the material and can be calculated using the predicted formula [9,39]:

$$H_v = 2 \left(\left(\frac{G}{B} \right)^2 G \right)^{0.585} - 3. \quad (2)$$

According to Pugh's empirical criterion, a solid can be classified as brittle if the $\frac{B}{G}$ ratio is less than the critical value of 1.75 and ductile if it is greater than the critical value. The $\frac{B}{G}$ ratio of the studied compound is 2.01, which reveals its elastic behavior, unlike the compared compound presented in table 5 because the bulk modulus B is twice that of the shear modulus G , indicating that shear strain is easier to occur in the test compound. In addition to the Pugh ratio, the ductile behaviour of the compound can be confirmed because its Poisson's ratio = 0.28 is greater than 0.26, which is considered a boundary between the ductile and brittle materials. On the other hand, the chemical bonds between neighbouring atoms can be classified as ionic if the Poisson's ratio is greater than the critical value of 0.25 and as covalent otherwise [40]. Regarding our compound, it is evident that the calculated value of the Poisson's ratio (0.286) is greater than 0.25, indicating the ionic bonding between the atoms, unlike the other compound in the same table

Table 2. Calculated structural parameters of the relaxed structure and energy of formation for Mn_2VSnC_2 compound along with compared results for the ternary V_3SnC_2 compound.

Compound	Phase		a (Å)	c (Å)	c/a	B (GPa)	E_{form} (eV/atom)
Mn_2VSnC_2	Alpha	NM	3.044	17.522	5.756	214.230	– 2.628
		FM	3.041	18.077	5.943	162.404	– 2.880
		AFM1	3.022	17.996	5.954	196.156	– 2.634
		AFM2	3.017	18.159	6.0185	169.794	– 2.657
		AFM3	2.997	18.467	6.161	160.939	– 2.645
	Beta	NM	3.038	18.904	6.220	200.278	– 2.775
		FM	3.003	19.021	6.333	219.417	– 2.790
		AFM1	3.260	16.520	5.067	183.810	– 2.809
		AFM2	3.265	16.547	5.067	170.187	– 2.580
	AFM3	3.034	19.112	6.297	185.0263	– 2.581	
V_3SnC_2 [23]	Alpha		3.0845	18.374	5.9569	1943278	– 2.979
	Beta		3.0671	19.456	6.3436	193.8133	– 2.671

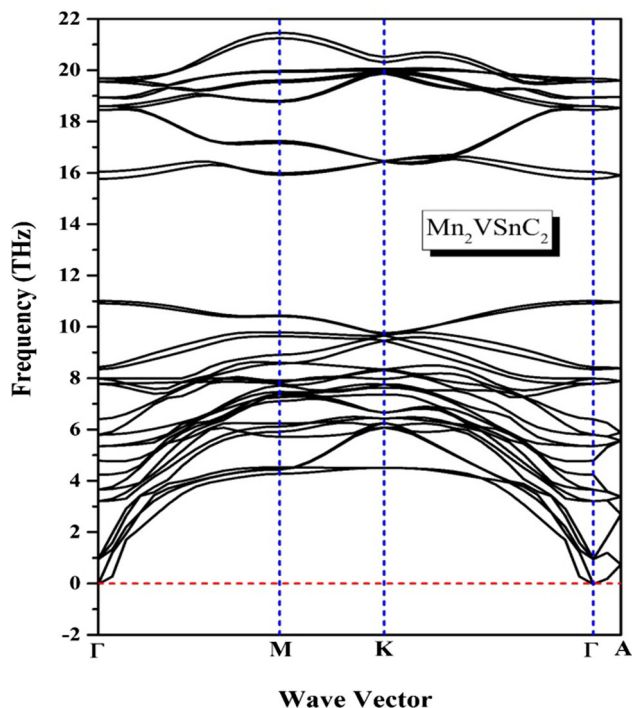


Figure 3. The obtained phonon band structures along the high symmetry directions in the first BZ.

(see table 5), where the covalent character of this material is dominant.

In addition, the Cauchy pressure P^{Cauchy} plays an important role in determining the nature of the chemical bonds, as it is classified as an ionic bond if it

Table 6. Computed shear anisotropic parameters (A_1 , A_2 , A_3) and K_c/K_a .

Compound	A_1	A_2	A_3	K_c/K_a
Mn_2VSnC_2	1.067	0.892	0.952	3.881
V_3SnC_2 [23]	0.922	1.075	0.993	1.797

has a positive sign and a covalent bond if it has a negative sign [9,17]. Even the negative sign implies the fragility of the behaviour of these substances, while the positive sign implies the flexibility of the behaviour [9,17]. Table 5 shows that all the P^{Cauchy} values are positive, indicating the ionic character and ductile behaviour of our compounds. All the results obtained by the three parameters, Pugh’s and Poisson’s ratios and Cauchy pressure, are identical, which allows us to say that our results are accurate and reliable.

The shear anisotropic factor A is also an extremely important parameter, mainly related to microcracks in crystal systems and is used to analyse the degree of durability of the materials. In a hexagonal system, there are three shear anisotropy factors, A_1 for the plane $\{1\ 0\ 0\}$ between the $[0\ 1\ 1]$ and $[0\ 1\ 0]$ directions, A_2 for the plane $\{0\ 1\ 0\}$ between the $[1\ 0\ 1]$ and $[0\ 0\ 1]$ directions and A_3 for the plane $\{0\ 0\ 1\}$ between the $[1\ 1\ 0]$ and $[0\ 1\ 0]$ directions [41]. The anisotropy factor K_c/K_a , which indicates in which direction the compound is more compressible, is defined as follows:

Table 3. Computed total, atomic and interstitial site magnetic moments (in Bohr magneton).

Compound	$M_{tot} (\mu_B)$	M_{atomic}				
		V (μ_B)	Mn (μ_B)	Sn (μ_B)	C (μ_B)	Interstitial (μ_B)
Mn_2VSnC	7.41261	0.08999	1.79270	− 0.0900	− 0.08239	0.40942

Table 4. Computed elastic constants (C_{ij} , in GPa).

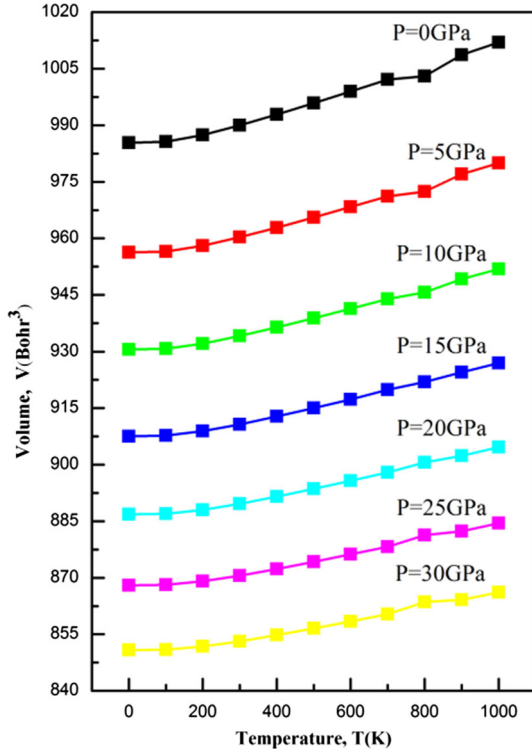
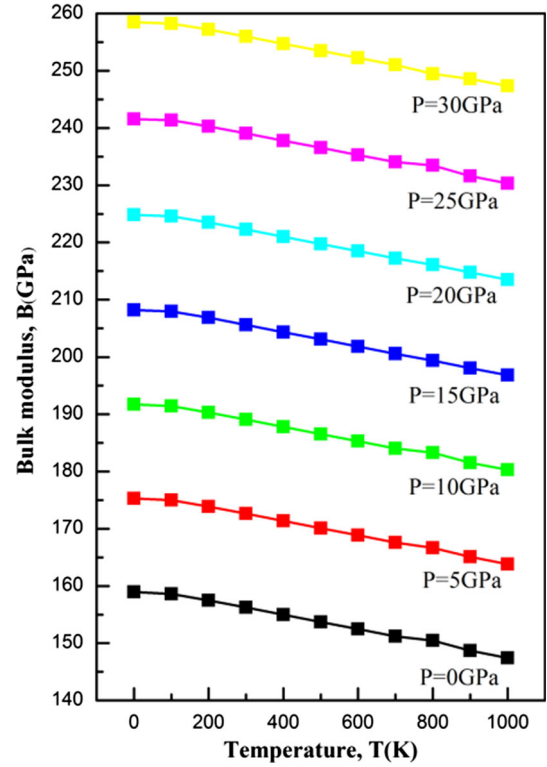
Compound	C_{11}	C_{33}	C_{12}	C_{13}	$C_{55} = C_{44}$	C_{66}
Mn_2VSnC_2	324.50	167.78	160.78	88.21	73.08	81.85
V_3SnC_2 [23]	324.23	255.60	161.07	127.60	87.77	81.58

Table 5. Computed elastic moduli (B , G and E ; in GPa), Poisson’s ratio (ν), G/B ratio, Vickers hardness (H_v in GPa) and Cauchy pressure.

Compound	B	G	B/G	E	H_v	ν	P_X^{Cauchy}	P_Z^{Cauchy}
Mn_2VSnC_2	153.21	76.16	2.01	196.00	8.134	0.286	15.12	78.92
V_3SnC_2 [23]	190.57	83.66	2.27	218.96	7.172	0.308	39.82	79.49

Table 7. Computed density, longitudinal, transverse and average elastic wave velocity [ρ (in g/cm^3), v_l , v_t , v_m (in m/s)], Debye temperatures (θ_D in K) and melting temperature (T_m in K)

Compound	ρ (g/cm^3)	v_l	v_t	v_m	θ_D	T_m
Mn_2VSnC_2	6.9606	6049.8	3307.81	3688.63	478.757	1579.17
V_3SnC_2 [23]	6.4836	6826.45	3592.32	4016.9	513.72	1710.12

**Figure 4.** The effects of temperature and pressure on the volume of Mn_2VSnC_2 .**Figure 5.** The effects of temperature and pressure on the bulk modulus of Mn_2VSnC_2 .

$$\frac{K_c}{K_a} = \frac{(C_{11} + C_{12} - 2C_{13})}{(C_{33} - C_{13})}$$

The predicted values of the shear anisotropic factors A_1 , A_2 and A_3 and of the compressibility anisotropy factor K_c/K_a of the Mn_2VSnC_2 compound are reported in table 6. According to these results, all shear anisotropy factors deviate from isotropic value criteria $A_i = 1$, indicating that the studied compound exhibits an anisotropy behaviour. The value of the compressibility anisotropy factor K_c/K_a is greater than 1, indicating that the c -axis is more compressible than the a -axis. It can be seen that the anisotropy factor results of the Mn_2VSnC_2 compound are in good agreement with the previous results for the V_3SnC_2 compound.

Debye temperature (θ_D) and the sound velocity v are important parameters in solid-state physics and it is associated with elasticity parameters, which express

the mechanical and thermodynamic properties of the materials. It can be estimated from the average velocity of sound suggested by Anderson [42]. The melting temperature T_m is also related to the elastic constants and allows us to study the purity of materials [43]. The calculated values of v , θ_D and T_m are given in table 7. From the listed values, it can be seen that both compounds have almost the same values. Also we can remark that both compounds have high values of melting and Debye temperatures, making them suitable for use in harsh environments.

5. Thermodynamic properties

To study the effects of temperature and pressure on various thermodynamic quantities of the compound, we

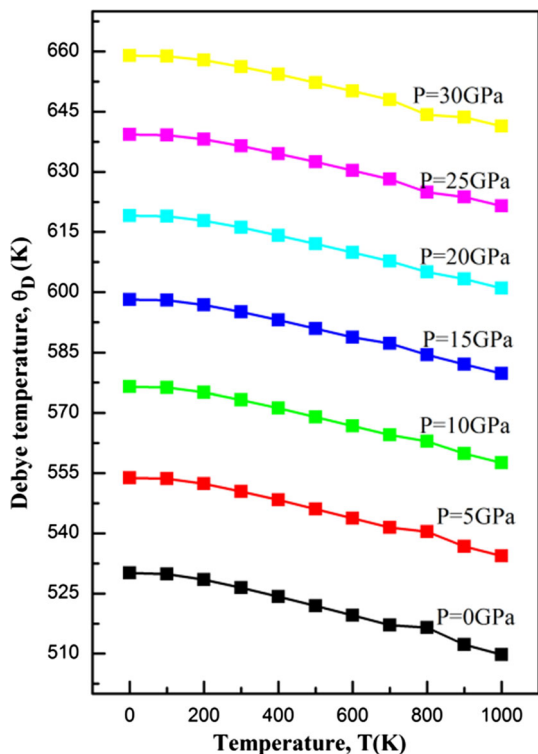


Figure 6. The effects of temperature and pressure on the Debye temperature of Mn_2VSnC_2 .

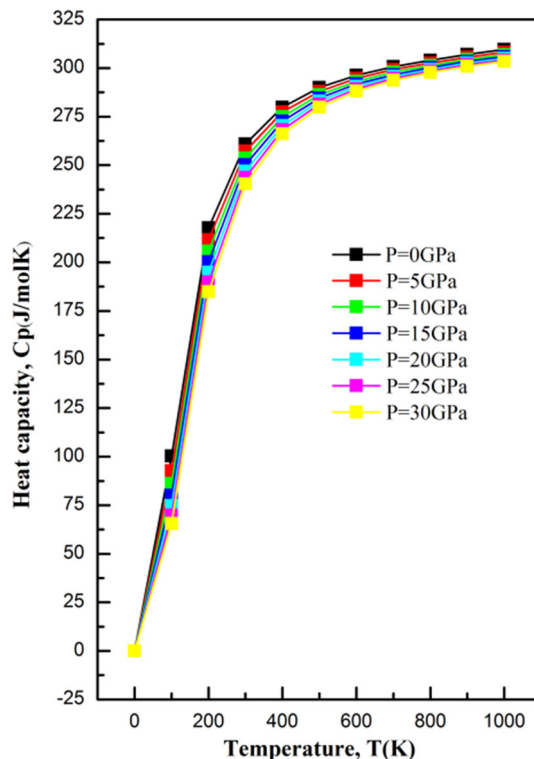


Figure 8. The effects of temperature and pressure on C_p of Mn_2VSnC_2 .

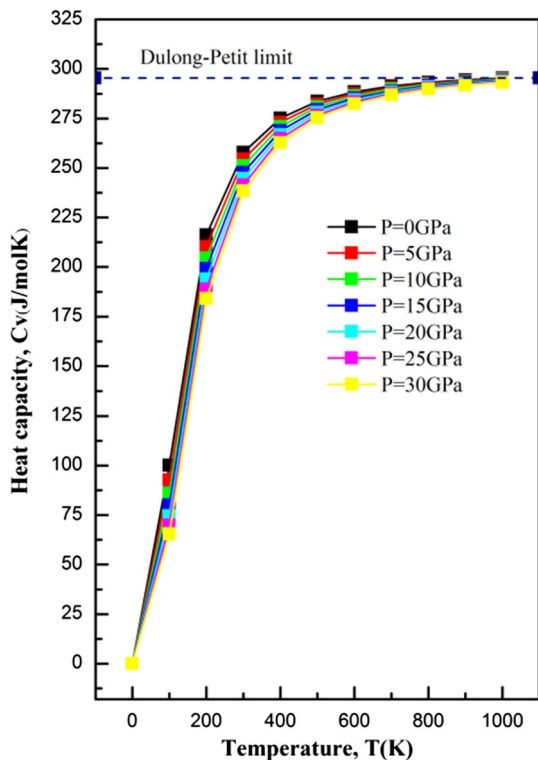


Figure 7. The effects of temperature and pressure on C_v of Mn_2VSnC_2 .

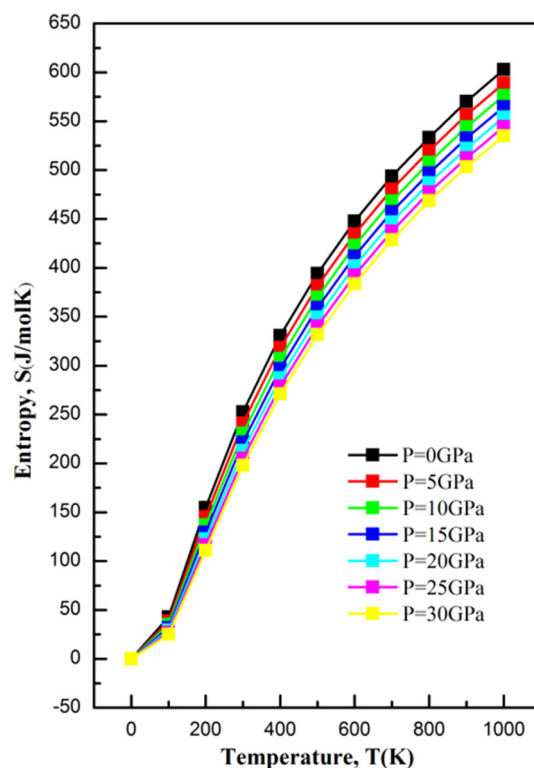


Figure 9. The effects of temperature and pressure on the entropy of Mn_2VSnC_2 .

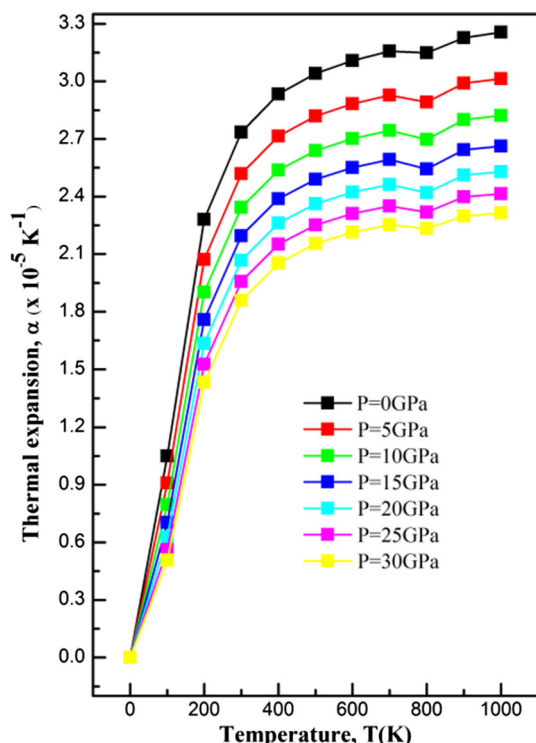


Figure 10. The effects of temperature and pressure on the thermal expansion coefficient of Mn_2VSnC_2 .

have employed the Gibbs2 package based on the quasi-harmonic model of Debye [44,45]. These effects were investigated in the temperature range of 0–450 K and the pressure range of 0–30 GPa. Further details about this calculation and the employed equations can be found in refs [46,47].

Figures 4 and 5 represent the evolution of the volume of the unit cell V and the bulk modulus B under the influence of both temperature and pressure. From figure 4, it can be observed that volume V improves slightly and linearly with the increasing temperature at constant pressures. On the contrary, V decreases with increasing pressure at a constant temperature. We notice that the volume is the greatest for 1000 K, 0 GPa and the lowest for 0 K, 30 GPa. On the contrary, and according to figure 5, increasing temperature decreases the bulk modulus B while increasing pressure increases its value. That is, there is an inverse relationship between volume, modulus and temperature and a linear relationship between B and pressure, where its value is the highest at 0 K, 30 GPa and the lowest at 1000 K, 0 GPa, according to the studied interval.

The value of θ_D indicates the bond strength in materials. Figure 6 shows the effects of pressure and temperature on θ_D for the Mn_2VSnC_2 compound. At fixed pressure, it can be seen that θ_D decreases with increasing temperature. The effect of pressure on θ_D is opposite to the effect of temperature. The heat

capacity at constant volume C_V and constant pressure C_P is closely related to the vibrational properties of the materials. The effects of temperature and pressure on C_V and C_P of Mn_2VSnC_2 are shown in figures 7 and 8. It can be observed from these figures that C_V or C_P changes in the same way. When the temperature is lower than 200 K, they increase rapidly with increasing temperature and then continue to increase slightly with increasing temperature. Figure 9 shows the effects of temperature and pressure on the entropy S for the Mn_2VSnC_2 compound. It is clear that S increases with increasing temperature and decreases with increasing pressure. We can also emphasise that S is more sensitive to temperature than to pressure. The thermal expansion α has also been studied by changing pressure and temperature. The effects of temperature and pressure on α for Mn_2VSnC_2 are shown in figure 10. When the temperature is less than 200 K, α increases almost linearly with the increase in temperature up to 300 K, then its intensity decreases with the increase in temperature. We see here that the effect of pressure is the inverse of the effect of temperature on α .

5.1 Electronic structure

In the following part, we analyse the electronic structures of the compound, which are considered extremely important and provide us with important information about the nature of the chemical bonds, electrical resistivity and electronic conductivity. Figure 11 shows the band structure of Mn_2VSnC_2 along with the high symmetry axes of the first BZ. It is clear that there is an overlap between the valence and conduction bands at the Fermi level E_F , i.e. there is no band gap at E_F , and as a result, this compound exhibits metallic nature like the previous compounds of this family, such as Zr_3AlC_2 and Ti_3AlC_2 [32].

We have also simultaneously analysed the total and the partial density of states (TDOS and PDOS). The calculated TDOS and PDOS are illustrated in figure 12. Their analysis confirms again the metallic nature of the compound, where the TDOS crosses E_F for both spin channels. Furthermore, we can segment the TDOS spectrum of the Mn_2VSnC_2 compound into four main regions. The first region is between -13 and -10.7 eV below E_F , where the s -(C) states are the most prevalent. The second region is confined between -7 and -3 eV below E_F . Here, the p -(C) and d -(V, Mn) states are the most dominant. The third region, also in the valence band, is between -3 and 0.0 eV. At this region, a strong hybridisation occurs between the p -(Sn) and d -(V, Mn) states, while the conduction band comes mainly from the ionic bonding between d -(V, Mn, Sn) and p -(C, Sn) states (figure 12).

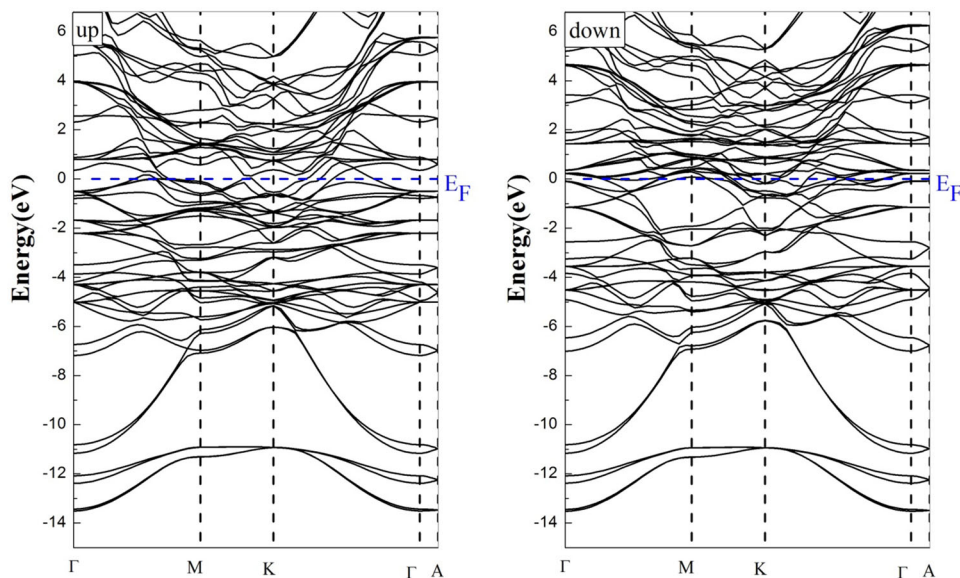


Figure 11. The calculated band structures of Mn_2VSnC_2 .

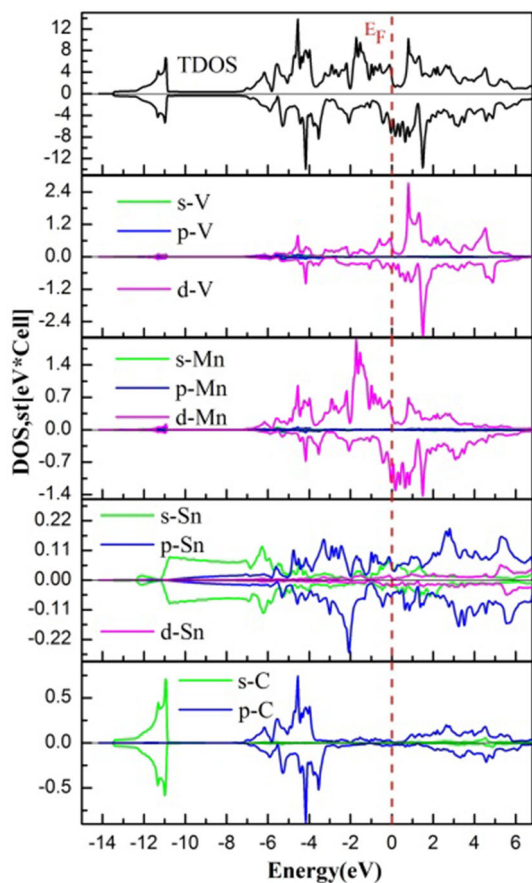


Figure 12. The calculated state densities of Mn_2VSnC_2 .

6. Conclusion

In summary of this research paper, the *ab-initio* calculation was employed to study the stability and

thermomechanical properties of the new MAX-phase compound Mn_2VSnC_2 . According to the equilibrium ground-state properties, Mn_2VSnC_2 was stable in α -polymorph ferromagnetic ordering. To obtain information on the thermodynamic stability, we calculated the formation energy, the negative sign of which ensures the thermodynamic stability of the compound. The independent elastic constants confirmed the mechanical stability of the compound against elastic deformation. Furthermore, the calculated macroscopic mechanical moduli revealed the ductile nature of the compound. Thermodynamic analysis indicated that the effect of pressure on the bulk modulus, Debye temperature, thermal expansion, entropy and heat capacity was greater than temperature. The results agreed with the reported outcomes for the compared ternary MAX-phase compound. In addition, the results revealed that this compound is a promising material for harsh environmental applications owing to its high melting and Debye temperatures. From the electronic structures, we found that Mn_2VSnC_2 exhibited metallic behaviour. Finally, we consider the present report to be the first quantitative theoretical prediction and we hope it will inspire new theoretical and experimental research on this compound.

Acknowledgements

The author acknowledge the funding provided by the Direction Générale de la Recherche Scientifique et du Développement Technologique (Grant No. B00L02UN220120190002).

References

- [1] T Lapauw *et al*, *J. Eur. Ceramic Soc.* **36**, 1847 (2016), <https://doi.org/10.1016/j.jeurceramsoc.2016.02.044>
- [2] W Jeitschko, H Nowotny and F Benesovsky, *Monatshefte Chem.* **94**, 672 (1963), <https://doi.org/10.1007/BF00913068>
- [3] M W Barsoum *et al*, *J. Am. Ceramic Soc.* **82**, 2545 (1999), <https://doi.org/10.1111/j.1151-2916.1999.tb02117.x>
- [4] C Hu *et al*, *Scr. Mater.* **57**, 893 (2007), <https://doi.org/10.1016/j.scriptamat.2007.07.038Get>
- [5] M W Barsoum, *MAX-Phases: Properties of machinable ternary carbides and nitrides* (Wiley-VCH, Weinheim Germany, 2013), <https://doi.org/10.1002/9783527654581>
- [6] M W Barsoum and T El-Raghy, *Am. Sci.* **89**, 334e343 (2001), <https://www.jstor.org/stable/27857502>
- [7] H I Yoo, M W Barsoum and T El-Raghy, *Nature* **407**, 581 (2000), <https://doi.org/10.1038/35036686>
- [8] M A Hadi *et al*, *Sci. Rep.* **11**, 3410 (2021), <https://doi.org/10.1038/s41598-021-81346-w>
- [9] A Azzouz-Rached *et al*, *Int. J. Quantum Chem.* **121**, e26770 (2021), <https://doi.org/10.1002/qua.26770>
- [10] M A Hadi, *J. Phys. Chem. Sol.* **138**, 109275 (2020), <https://doi.org/10.1016/j.jpccs.2019.109275>
- [11] A Azzouz-Rached *et al*, *J. Alloy Compd.* **885**, 160998 (2021), <https://doi.org/10.1016/j.jallcom.2021.160998>
- [12] A A Belkacem *et al*, *Results Phys.* **38**, 105621 (2022), <https://doi.org/10.1016/j.rinp.2022.105621>
- [13] Y Rached *et al*, *Phys. Status Solidi B* **259**, 2200195 (2022), <https://doi.org/10.1002/pssb.202200195>
- [14] A Mockute *et al*, *Phys. Rev. B* **87**, 094113 (2013), <https://doi.org/10.1103/PhysRevB.87.094113>
- [15] A Mockute *et al*, *Phys. Status Solidi B*, 420 (2014), <https://doi.org/10.1002/pssr.201409087>
- [16] A Petruhins *et al*, *J. Mater. Sci.* **50**, 4495 (2015), <https://doi.org/10.1007/s10853-015-8999-8>
- [17] I P Novoselova *et al*, *Mater. Res. Lett.* **7**, 159 (2019), <https://doi.org/10.1080/21663831.2019.1570980>
- [18] R Meshkian *et al*, *APL Mater.* **3**, 076102 (2015), <https://doi.org/10.1063/1.4926611>
- [19] R Salikhov *et al*, *J. Appl. Phys.* **121**, 163904 (2017), <https://doi.org/10.1063/1.4982197>
- [20] Q Tao *et al*, *APL Mater.* **4**, 086109 (2016), <https://doi.org/10.1063/1.4961502>
- [21] P Blaha *et al*, *The J. Chem. Phys.* **152**, 074101 (2020), <https://doi.org/10.1063/1.5143061>
- [22] P Hohenberg and W Kohn, *Phys. Rev. B* **136**, 864 (1964), <https://doi.org/10.1103/PhysRev.136.B864>
- [23] J P Perdew and Y Wang, *Phys. Rev. B* **46**, 12947 (1992), <https://doi.org/10.1103/PhysRevB.46.12947>
- [24] H J Monkhorst and J D Pack, *Phys. Rev. B* **13**, 5188 (1976), <https://doi.org/10.1103/PhysRevB.13.5188>
- [25] A Azzouz-Rached *et al*, *Mater. Today Comm.* **27**, 102233 (2021), <https://doi.org/10.1016/j.mtcomm.2021.102233>
- [26] Y Rached *et al*, *Int. J. Quantum Chem.* e26875 (2021), <https://doi.org/10.1002/qua.26875>
- [27] H Rached, *Int. J. Quantum Chem.* **121**, e26647 (2021), <https://doi.org/10.1002/qua.26647>
- [28] S Baroni, S De Gironcoli, A Dal Corso and P Giannozzi, *Rev. Mod. Phys.* **73**, 515 (2001)
- [29] M D Segall *et al*, *J. Phys.: Condens. Matter* **14**, 2717 (2002)
- [30] B Montanari and N M Harrison, *Chem. Phys. Lett.* **364**, 528 (2002)
- [31] M Jamal *et al*, *J. Alloys Compd* **735**, 569(2018), <https://doi.org/10.1016/j.jallcom.2017.10.139>
- [32] I Ouadha *et al*, *Comput. Condens. Matter* **23**, e00468 (2020), <https://doi.org/10.1016/j.cocom.2020.e00468>
- [33] A Azzouz-Rached *et al*, *Mater. Chem. Phys.* **260**, 124189 (2021), <https://doi.org/10.1016/j.matchemphys.2020.124189>
- [34] F Mouhat and F-X Coudert, *Phys. Rev. B* **90**, 224104 (2014), <https://doi.org/10.1103/PhysRevB.90.224104>
- [35] W Voigt, *Lehrbuch der Kristallphysik* (Taubner, Leipzig, 1928)
- [36] A Reuss, *J. Appl. Math. Mech.* **9**, 49 (1929), <https://doi.org/10.1002/zamm.19290090104>
- [37] R Hill, *Proc. Phys. Soc. A* **65**, 349 (1952), <https://doi.org/10.1088/0370-1298/65/5/307>
- [38] H Rached, S Bendaoudia and D Rached, *Mater. Chem. Phys.* **193**, 453 (2017), <https://doi.org/10.1016/j.matchemphys.2017.03.006>
- [39] Y Tian, B Xu and Z Zhao, *Int. J. Refractory Metals Hard Mater.* **33**, 93 (2012), <https://doi.org/10.1016/j.ijrmhm.2012.02.021>
- [40] A Yildirim, H Koc and E Deligoz, *Chin. Phys. B* **21**, 037101 (2012), <https://doi.org/10.1088/1674-1056/21/3/037101>
- [41] H M Ledbetter, *J. Phys. Chem. Ref. Data* **6**, 1181 (1977), <https://doi.org/10.1063/1.555564>
- [42] O L Anderson, *J. Phys. Chem. Solidi* **24**, 909 (1963), [https://doi.org/10.1016/0022-3697\(63\)90067-2](https://doi.org/10.1016/0022-3697(63)90067-2)
- [43] M E Fine, L D Brown and H L Marcus, *Scr. Metall.* **18**, 951 (1984), [https://doi.org/10.1016/0036-9748\(84\)90267-9](https://doi.org/10.1016/0036-9748(84)90267-9)
- [44] A Otero-de-la-Roza, D Abbasi-Pérez and V Luaña, *Comput. Phys. Commun.* **182**, 2232 (2011), <https://doi.org/10.1016/j.cpc.2011.05.009>
- [45] R Fox, *the British J. History Sci.* **4**, 1 (1968), <https://doi.org/10.1017/S0007087400003150>
- [46] I Asfour, H Rached, S Benalia and D Rached, *J. Alloys Compds* **676**, 440 (2016), <https://doi.org/10.1016/j.jallcom.2016.03.075>
- [47] M E A Belhadj, H Rached, D Rached and S Amari, *Comput. Condensed Matter* **16**, e00295 (2018), <https://doi.org/10.1016/j.cocom.2018.e00295>